

The crystal structure of the RsbN– σ^{BldN} complex from *Streptomyces venezuelae* defines a new structural class of anti- σ factor

Maria A. Schumacher^{1,*}, Matthew J. Bush², Maureen J. Bibb², Félix Ramos-León², Govind Chandra², Wenjie Zeng¹ and Mark J. Buttner^{2,*}

¹Department of Biochemistry, Duke University School of Medicine, Durham, NC 27710, USA and ²Department of Molecular Microbiology, John Innes Centre, Norwich Research Park, Norwich NR4 7UH, UK

Received January 15, 2018; Revised May 13, 2018; Editorial Decision May 18, 2018; Accepted May 24, 2018

ABSTRACT

Streptomyces are filamentous bacteria with a complex developmental life cycle characterized by the formation of spore-forming aerial hyphae. Transcription of the *chaplIn* and *rodlin* genes, which are essential for aerial hyphae production, is directed by the extracytoplasmic function (ECF) σ factor BldN, which is in turn controlled by an anti- σ factor, RsbN. RsbN shows no sequence similarity to known anti- σ factors and binds and inhibits BldN in an unknown manner. Here we describe the 2.23 Å structure of the RsbN–BldN complex. The structure shows that BldN harbors σ_2 and σ_4 domains that are individually similar to other ECF σ domains, which bind –10 and –35 promoter regions, respectively. The anti- σ RsbN consists of three helices, with α_3 forming a long helix embraced between BldN σ_2 and σ_4 while RsbN α_1 – α_2 dock against σ_4 in a manner that would block –35 DNA binding. RsbN binding also freezes BldN in a conformation inactive for simultaneous –10 and –35 promoter interaction and RNAP binding. Strikingly, RsbN is structurally distinct from previously solved anti- σ proteins. Thus, these data characterize the molecular determinants controlling a central *Streptomyces* developmental switch and reveal RsbN to be the founding member of a new structural class of anti- σ factor.

INTRODUCTION

Bacterial transcription is driven by an evolutionarily conserved catalytic RNA polymerase (RNAP) that consists of five subunits, $\alpha_2\beta\beta'\omega$. This core enzyme must associate with one of several dissociable transcription initiation factors called sigma (σ) factors to elicit promoter-specific transcrip-

tion (1,2). Transcription of most genes is driven by the primary σ factor (called σ^{70} in *Escherichia coli*) but alternative σ factors redirect transcription to smaller regulons of genes, allowing bacteria to mount specific responses to discrete environmental and internal cues (1,3,4). σ factors are modular proteins having up to four conserved globular domains (σ_{1-4}) with distinct functions (5). The –10 and –35 promoter elements are recognized and bound by σ_2 and σ_4 , respectively (1,6–13), whereas the interface that interacts with RNAP is extensive, involving σ_2 , σ_3 and σ_4 (1,10,13).

The most abundant and phylogenetically diverse class of σ factors is the extracytoplasmic function (ECF) σ factor subfamily, so-called because more than 80% of these proteins regulate physiological functions in response to stimuli arising outside the cytoplasmic membrane (14–18). These σ factors have also been termed group IV σ factors (3). Structurally, these proteins are the most reduced σ factors, consisting only of σ_2 and σ_4 connected by a linker (12,14,15,18). It is typical for bacteria to express these σ factors but to hold them in an inactive form until appropriate stimuli trigger their release, permitting a rapid response to the relevant signal. This inhibition is achieved through the action of anti- σ factors, proteins that bind their cognate σ factors and prevent them from interacting with RNAP (1,16–21). Very often ECF anti- σ factors are transmembrane proteins that sequester σ to the lipid bilayer, with their extracytoplasmic domain directly or indirectly receiving the signal that ultimately leads to release of σ on the cytoplasmic side of the membrane (1,16–21).

To date, several ECF σ –anti- σ complexes have been structurally characterized, including the *E. coli* RseA– σ^{E} , *Rhodobacter sphaeroides* ChrR– σ^{E} , *Bacillus subtilis* RsiW– σ^{W} and *Mycobacterium tuberculosis* RskA– σ^{K} complexes (22–25). Interestingly, although the anti- σ factors in these structures show limited sequence similarity, they contain a conserved fold consisting of a three-helix bundle followed by a fourth helix of variable position (22–25). In all these

*To whom correspondence should be addressed. Tel: +1 919 684 9468; Fax +1 919 684 8888; Email: maria.schumacher@duke.edu
Correspondence may also be addressed to Mark J. Buttner. Tel: +44 1603 450759; Fax: +44 1603 450045; Email: mark.buttner@jic.ac.uk

structures, this anti- σ factor domain (ASD) locks the σ factor in a non-optimal position for promoter docking and prevents its interaction with RNAP and DNA. More recent structural studies on the anti- σ factors NepR and CnrY revealed these proteins to be composed of just two helices that act as a clamp to embrace the outer surface of their partner proteins to inhibit their activity (26–28). CnrY binds the σ factor, CnrH, while the NepR protein is involved in a partner switching mechanism wherein it can bind either the σ factor EcfG or the phosphorylated form of the σ factor mimic, PhyR. While a structure of an NepR–EcfG complex has not yet been solved, NepR–PhyR structures suggest this complex mimics the NepR–EcfG complex. In the NepR–PhyR complex, similar to CnrY, NepR forms a two-helix clamp that encircles the surface of PhyR (27,28). Thus, structural studies to date have revealed two ECF anti- σ factor folds.

The structures of σ –anti- σ complexes also show that the individual σ_2 and σ_4 domains of the ECF σ factors adopt essentially the same fold, which are similar to the corresponding domains of the larger primary σ^{70} proteins (22–28). The σ_4 domains bind the –35 promoter element via a helix-turn-helix (HTH) motif and the σ_2 domains use a loop to recognize and melt out the –10 motif of the promoter. Structures of ECF σ domains bound to cognate –10 and –35 sequences reveal that, in general, they dock onto DNA in a similar fashion to the corresponding domains in σ^{70} proteins (1,6,8,12). However, ECF σ_2 domains mediate single base flipping events within their target –10 elements compared to the double base exposure exhibited by primary σ factors. In addition, ECF σ_4 domains appear to bind more tightly and specifically to their –35 elements than primary σ factors (1).

ECF σ –anti- σ modules provide a rapid and modular readout of stress responses in bacteria, and they are now recognized as one of the three major pillars of signal transduction in bacteria (16–17). Most bacteria possess multiple ECF σ factors and in general bacteria with large genomes have larger numbers of ECF σ factors. Indeed, members of the genus *Streptomyces* typically have ~9 Mb genomes and ~50 ECF σ factors. These filamentous bacteria have a complex developmental life cycle that ultimately leads to the formation of long chains of exospores. During development, *Streptomyces* also produce a plethora of secondary metabolites, which serve as important sources of antibiotics and other clinically important agents such as anti-cancer and anti-fungal drugs (29,30). Most ECF σ factors that have been characterized function in environmental or endogenous stress responses, but in *Streptomyces* the ECF σ factor BldN plays a key role in morphological development (31). Specifically, the *bldN* gene is a direct target of the master transcriptional regulator, BldD, which sits at the top of the *Streptomyces* developmental hierarchy (Figure 1). Recent studies showed that c-di-GMP levels control BldD activity by mediating dimerization of two BldD subunits. BldD-c-di-GMP dimers drive repression of the large BldD regulon of sporulation genes, extending vegetative growth and blocking the onset of morphological differentiation (31–33). When c-di-GMP levels drop, the BldD dimer falls apart and dissociates from the DNA, which allows the production of BldN. The BldN protein plays a pivotal role in the on-

set of development by directing transcription of the *rodlin* and *chaplin* genes (31), which encode the proteins required to form an external hydrophobic sheath that permits the reproductive aerial hyphae to escape surface tension and grow into the air (Figure 1). These proteins also likely prevent the desiccation of the aerial hyphae, which undergo a massive synchronous septation event to form chains of exospores for dispersal (34–40).

A second key direct target of BldD-(c-di-GMP)-mediated repression is the promoter of the *rsbN* gene (Figure 1), which is a direct target of BldN. We previously showed that RsbN functions as a BldN-specific anti- σ factor, and that deletion of *rsbN* triggers precocious development, emphasizing the importance of this post-translational level of BldN regulation (31). RsbN is a transmembrane protein, having a single transmembrane helix (residues 118–139) that connects a 117 residue N-terminal cytoplasmic region to a 272 amino acid C-terminal extracytoplasmic domain (Figure 1) (31). RsbN does not show sequence similarity to any known anti- σ factor or, indeed, any known protein. To discover how RsbN binds the key developmental regulator BldN, we determined the crystal structure of the complex between BldN and the cytoplasmic anti- σ factor domain of RsbN. The structure reveals how RsbN inhibits BldN and also identifies RsbN as the founding member of a new structural class of anti- σ factor.

MATERIALS AND METHODS

Purification of RsbN–BldN

We previously showed that full length RsbN interacts directly with BldN (31). Subsequent limited proteolysis analyses revealed that the minimal BldN-interacting region of RsbN consists of residues 1–91. Thus, for structural studies *bldN* and *rsbN*(1–91) were cloned into the pETDuet-1 vector for coexpression and purified as a single complex. The resultant complex was >95% pure after a cobalt-nitrilotriacetic acid column chromatography step and was used for crystallization trials. Large crystals of the complex (at a concentration of 80 mg/ml) were obtained via hanging drop vapor diffusion using 30% polyethylene glycol (PEG) 3350, 0.2 M ammonium sulphate as a crystallization reagent. However, the crystals diffracted weakly to 8 Å and were significantly twinned. As previous studies on σ –anti- σ factors showed that the linker between the σ factor domains is flexible, we generated a system in which RsbN(1–91) was expressed with individual BldN domains (domain 2 and domain 4). In this expression system, his-tagged RsbN91 and non-tagged BldN domain 2 (σ_2) were expressed from pCOLADuet-1 (pIJ10626), and non-tagged BldN domain 4 (σ_4) was expressed from pET15b (pIJ10622) (Supplementary Table S1). For protein expression of this system, both plasmids were transformed into C41(DE3) cells and grown in Luria-Bertani (LB) liquid medium to an OD₆₀₀ of 0.6 and induced with 1 mM isopropyl β -D-1 thiogalactopyranoside (IPTG) for 3 h at 30 °C. The cells were then suspended in buffer A (25 mM Tris pH 7.5, 5% glycerol, 300 mM NaCl) and disrupted with a microfluidizer. The lysate was loaded onto a cobalt-nitrilotriacetic acid column. The his-RsbN(1–91) bound both non-tagged BldN σ domains and

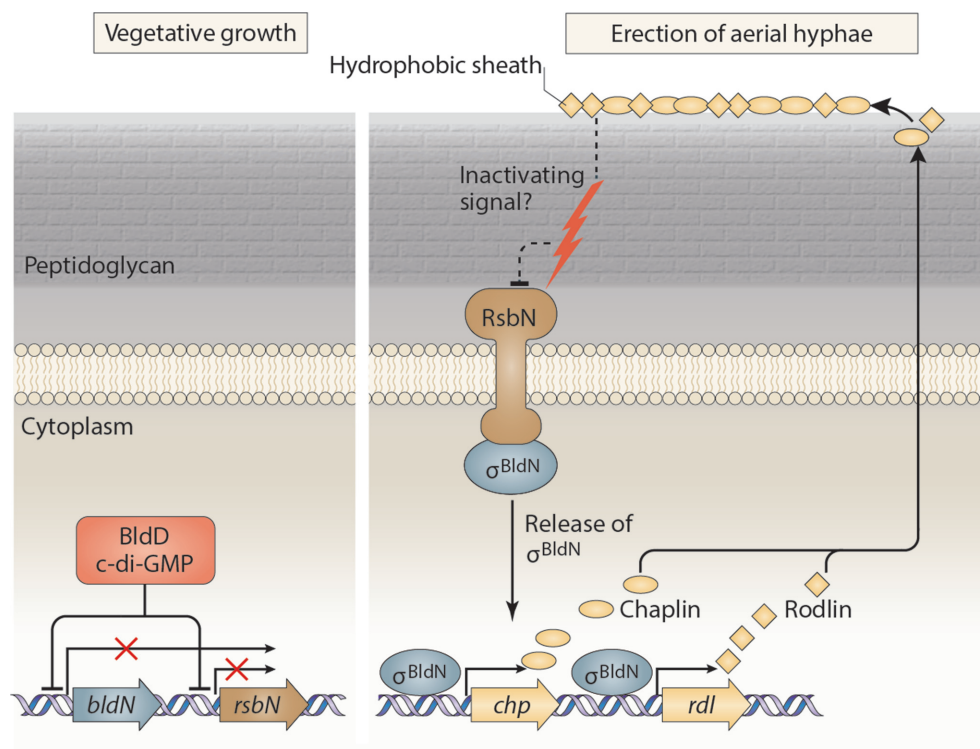


Figure 1. The biological role of BldN and RsbN. During vegetative growth, transcription from the *bldN* and *rsbN* promoters is repressed by the BldD–(c-di-GMP) complex. At the onset of development, c-di-GMP levels drop and BldD repression is relieved. As a consequence, BldN and RsbN are expressed and RsbN sequesters BldN to the membrane via its cytoplasmic anti- σ domain. In response to an unknown signal, RsbN releases BldN, which directs transcription of the two gene families encoding the chaplins and the rodlin, and these proteins assemble into functional amyloids to form the external hydrophobic sheath that allows the reproductive aerial hyphae to escape surface tension and grow into the air.

the ternary complex was eluted using increasing concentrations of imidazole in buffer A. For protein used for crystallization trials, an additional size exclusion chromatography (SEC) purification step was included. The protein complex was >97% pure after this step. The purified protein complex from this expression system produced well diffracting crystals that were used for structure determination.

Crystallization and structure determination of the BldN(σ_2)–BldN(σ_4)–RsbN(1–91) complex

Prior to crystallization, the RsbN his-tag was removed from the RsbN(1–91) that was in complex with BldN(σ_2)–BldN(σ_4) using a thrombin capture cleavage kit (Qiagen). Following thrombin treatment, the BldN(σ_2)–BldN(σ_4)–RsbN(1–91) complex was concentrated to 50 mg/ml using 30 kDa cutoff microcon concentrators, which simultaneously concentrated the complex and removed the cleaved his-tag. Crystals were obtained of the concentrated complex using hanging drop vapor diffusion. Specifically, the complex was mixed 1:1 with a crystallization solution consisting of 0.2 M ammonium nitrate, 26% PEG 3500 and placed over a 1 ml well containing the crystallization solution. Crystals were obtained at room temperature (RT) and took one week to grow to maximum size. The crystals were cryo-preserved by a 1–2 s dip in the crystallization solution supplemented with 10–20% glycerol. An x-ray intensity dataset was collected at the Advanced Light Source (ALS) beamline 8.3.1, the data were processed in

MOSFLM (41) and scaled using SCALA (42). Molecular replacement was used to solve the structure using a multi-step strategy. First, the σ_4 domain from *E. coli* σ^{70} (PDB ID: 2P7V) (43) was employed as a search model and produced a clear solution in Molrep. This partial model was then used as a static structure to obtain a solution of the σ_2 domain from CnrH (PDB ID: 4CXF) (26). The model was subjected to refinement in Phenix to 2.6 Å (44). After several rounds of refinement, rebuilding and replacement of the BldN sequence (45), density for RsbN α_3 was evident and built as a polyaniline model. Following several more rounds of refinement, RsbN α_1 – α_2 became clear and the sequence was evident for all residues in the RsbN helices. After several more rounds of rebuilding and solvent addition with concomitant analyses using Molprobit (46) the $R_{\text{work}}/R_{\text{free}}$ converged to 19.2/23.5% to 2.23 Å resolution (Table 1). The clashscore and overall score from Molprobit place the structure in the 99% range of structures solved to similar resolutions (46). The final model includes residues 2–80, 114–172 of BldN, RsbN residues 4–21, 39–79 and 72 water molecules.

Size exclusion chromatography (SEC) analysis of WT RsbN–BldN

SEC was used to probe the MW of the RsbN–BldN complex with a HiLoad 26/600 Superdex 75 prep grade column. Experiments were performed in a buffer containing 200 mM NaCl, 5% glycerol, 20 mM Tris HCl pH 7.5 and 1 mM

Table 1. Data collection and refinement statistics for the RsbN–BldN structure

| Structure | RsbN–BldN |
|---------------------------------------|---------------------|
| PDB code | 6C03 |
| Space Group | P2 ₁ |
| Cell dimensions | |
| a,b,c (Å) | 44.88, 43.58, 58.75 |
| α,β,γ (°) | 90, 111.56, 90 |
| Resolution (Å) | 34.5–2.23 |
| Total reflections, # | 23950 |
| Unique reflections, # | 9444 |
| R_{sym} | 0.108 (0.208)* |
| R_{pim} | 0.077 (0.190) |
| CC(1/2) | 0.908 (0.889) |
| I/ σ I | 6.5 (2.9) |
| Completeness (%) | 99.4 (70.1) |
| Redundancy | 2.5 (1.8) |
| Refinement | |
| Resolution (Å) | 34.5–2.23 |
| $R_{\text{work}}/R_{\text{free}}$ (%) | 19.2/23.5 |
| RMS deviations | |
| Bond lengths (Å) | 0.003 |
| Bond angles (°) | 0.678 |
| Ramachandran analyses | |
| Favored (%) | 98.4 |
| Disallowed (%) | 0.0 |

*Values in parentheses are for highest resolution shell.

β -mercaptoethanol (BME). For SEC analysis, the RsbN–BldN complex was loaded at a concentration of 10 μ M.

Biochemical analyses of truncated RsbN–BldN complexes

To further dissect the RsbN–BldN complex, we created a series of constructs to co-express truncated versions of BldN and RsbN, using the pCOLADuet-1 vector backbone (Supplementary Table S1). Plasmids were introduced into BL21(DE3) Rosetta-plysS and the resulting strains were grown in LB liquid medium to an OD₆₀₀ of 0.6 and induced with 1 mM IPTG for 2–3 h at 30°C. Cell pellets were suspended in buffer A, lysed by homogenization (two passes) using the Avestin Emulsiflex-B15 and the insoluble material was removed by centrifugation. Lysates were loaded onto 1 ml HiTrap columns (GE Healthcare) charged with 100 mM CoCl₂ and proteins were eluted using Buffer A + 500 mM imidazole. Representative fractions were run on a 16% Tricine gel (47), designed to resolve low MW proteins, and stained with Coomassie Brilliant Blue. The identity of each eluted protein was confirmed by MALDI-MS.

Analysis of site-directed mutants to probe the RsbN–BldN interaction

To test the effect of replacing key residues that the structure implied would be important for complex formation, we generated RsbN91(L70R) and RsbN91(F14R–L50R) mutants and assessed their abilities to interact with BldN σ_2 and BldN σ_4 , respectively. Specifically, RsbN91(L70R) was co-expressed with BldN σ_2 and RsbN91(F14R–L50R) was co-expressed with BldN σ_4 (Supplementary Table S1). Proteins were co-expressed in *E. coli* as above but instead purified using HIS-select spin columns (Sigma H7787) and run on 16% Tricine gels (47) for visualization with Coomassie Brilliant Blue.

To probe the BldN σ_4 –RsbN α_3 interaction, a co-expression system in which the wild-type (WT) full length BldN and a fusion construct consisting of the maltose binding protein (MBP) connected via a linker (SHSGGGSGGGGS) to RsbN α_3 (herein termed MBP–RsbN α_3) were encoded in pETDuet-1 (Supplementary Table S1). For protein expression, the plasmid was transformed into C41(DE3) cells and grown in LB to an OD₆₀₀ of 0.6 and induced with 1 mM IPTG for 3 h at 28°C. The cells were suspended in buffer A, disrupted with a microfluidizer and the lysate mixed with cobalt-nitrotriacetic acid resin. Protein containing fractions were then applied (at a concentration of 10 μ M) to a HiLoad 26/600 Superdex 75 column in buffer A.

RESULTS

Structure of *Streptomyces venezuelae* RsbN–BldN complex

We previously showed that *Streptomyces venezuelae* BldN formed a stable complex with the full-length 412 residue RsbN protein (31). Further analysis showed that an N-terminal 91 residue cytoplasmic domain of RsbN (RsbN91) was sufficient to mediate the interaction with BldN. Because BldN shows reduced solubility in the absence of RsbN (31), we constructed co-expression systems for structural studies. Crystals were obtained of full-length BldN in complex with RsbN91 but they did not diffract beyond 8 Å resolution. We speculated that this might be due to the long, 27-residue flexible linker connecting σ_2 and σ_4 of BldN. The length of this linker is similar to those found in other ECF σ factors (22–26). For example, the linkers in *E. coli* σ^E , *M. tuberculosis* σ^K , *B. subtilis* σ^W and CnrH, which range from 26 to 32 residues in length, are disordered in the σ^K , σ^W and CnrH structures in complex with their anti- σ factors and mostly disordered in the structure of σ^E bound to its anti- σ factor, RseA (22,24,25). Therefore, we generated a three-component co-expression system (‘Materials and Methods’ section) that produced RsbN91 and the σ_2 and σ_4 domains of BldN as three separate polypeptides. The protein complex purified from this system (herein referred to as RsbN–BldN) produced well diffracting crystals. Data were collected to 2.23 Å resolution, the structure solved by molecular replacement and refined to final $R_{\text{work}}/R_{\text{free}}$ values of 19.2/23.5% (‘Materials and Methods’ section and Table 1).

The structure shows that RsbN is composed of three helices that are bound to both the σ_2 and σ_4 domains of BldN (Figure 2A–D). The three RsbN helices are connected by flexible linkers. This flexibility is underscored by the finding that in the structure the linker between helices 2 and 3 domain swaps, which leads to helices 1–2 contacting a neighboring BldN σ_4 region in the crystal (Figure 2B). Domain swapping is an event in which a protein subunit exchanges a domain or part of its structure with an identical partner. This exchange requires a flexible connection between domains and generally occurs at high protein concentrations. The resultant swapped subunits have the identical structures as the unswapped subunit except for the flexible hinge region that connects the exchanging parts. This behaviour is significantly enhanced by certain kinds of hinge sequences in proteins that have been identified as hot-spots

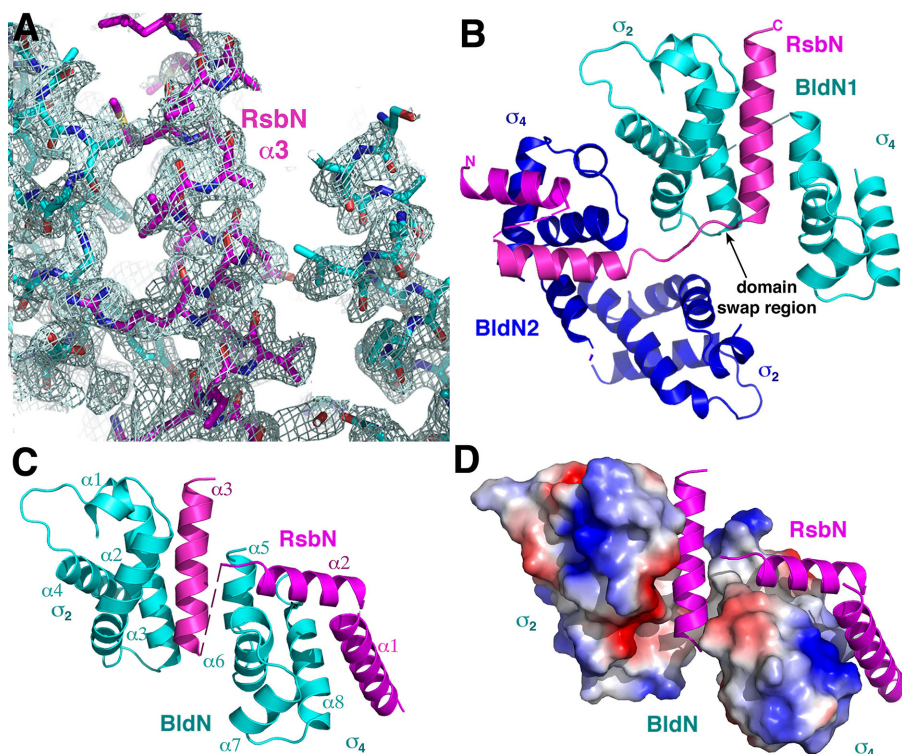


Figure 2. Crystal structure of the *Streptomyces venezuelae* RsbN-BldN complex. (A) 2Fo-Fc map (light blue mesh) contoured at 1 σ of the RsbN-BldN structure before addition of RsbN residues. Shown is a region around RsbN $\alpha 3$ (magenta). BldN residues are colored cyan. (B) Overall structure of RsbN-BldN. RsbN is colored magenta, one subunit of BldN is cyan and the other is blue. The asymmetric unit consists of one RsbN and one BldN subunit; however the RsbN molecule undergoes domain swapping leading to interaction of RsbN $\alpha 3$ with one BldN and RsbN $\alpha 1$ - $\alpha 2$ with another. Symmetry generation leads to an infinite array of RsbN-BldN complexes. (C) RsbN-BldN structure consistent with solution data showing that one subunit of RsbN contacts one BldN with RsbN $\alpha 3$ encircled by both BldN subunits and RsbN $\alpha 1$ - $\alpha 2$ interacting with BldN $\sigma 4$. (D) Electrostatic surface representation of BldN (shown in same orientation as panel C) bound to RsbN (shown as magenta cartoon). Electronegative and positive regions are colored red and blue, respectively, of the BldN surface. Note the hydrophobic (shown in white) nature of the RsbN interacting regions in BldN.

for domain swapping (48). The program H-Predictor quantifies for each residue in a protein the propensity to form such a hinge region (48). Strikingly, H-predictor identified the residues PKP in the linker between RsbN helices 2 and 3 as having an extremely high probability to form a hinge region that would be involved in domain swapping (Supplementary Figure S1), exactly reflecting what we observed in the crystal structure. As noted, domain swapping is also promoted by high protein concentration (48) and to obtain crystals, set-ups had to be performed using RsbN-BldN at 50 mg/ml. To assess the oligomeric state of the complex in solution, we performed SEC. If the domain-swapped structure exists in solution it would produce an indefinitely large polymer as each RsbN contacts successive BldN subunits (Supplementary Figure S2A). However, if the complex is as shown in Figure 2C, the MW obtained from the SEC experiment should be consistent with a 1:1 complex (with a calculated MW of 33 kDa). The SEC experiment revealed a MW of 39 kDa, supporting that RsbN-BldN exists as a 1:1 complex in solution (Supplementary Figure S2B).

In the structure, the BldN $\sigma 2$ domain is composed of helices 1-4, and the $\sigma 4$ domain is composed of helices 5-8, with helices 7 and 8 forming an HTH motif. Structural homology searches (DALI) with the RsbN-BldN structure revealed that the BldN $\sigma 2$ and $\sigma 4$ domains individually show

significant structural homology with multiple σ factors. In particular, BldN $\sigma 2$ and $\sigma 4$ superimpose on *E. coli* σ^E_2 and *M. tuberculosis* σ^K_4 with root mean squared deviations (rmsds) of 1.13 Å and 1.06 Å for 73 and 57 corresponding C α atoms, respectively. However, no σ factor aligns with both BldN domains simultaneously, indicating that the relative orientation of the two domains in the RsbN-BldN complex is different from those found in other σ factor structures. This is not unexpected as $\sigma 2$ and $\sigma 4$ are flexibly attached domains and structures show that they adopt different arrangements relative to each other when bound to anti- σ factors or RNAP (1). In the RsbN-BldN structure there is only one contact between $\sigma 2$ and $\sigma 4$, which is between $\sigma 2$ residue Glu41 and $\sigma 4$ residue Arg123 (Figures 2D and 3A). Notably, unlike BldN, no structures with any homology to RsbN were detected, using either the domain swapped or non-swapped conformations.

RsbN-BldN interface

The RsbN-BldN interface revealed in the structure is extensive and can be divided into three contact regions. Two of the contact regions are formed by the interaction of RsbN helix 3 ($\alpha 3$) with residues from the BldN $\sigma 2$ and $\sigma 4$ domains. The combined interface formed by these interactions buries 2510 Å² of protein surface from solvent. Indeed, RsbN $\alpha 3$

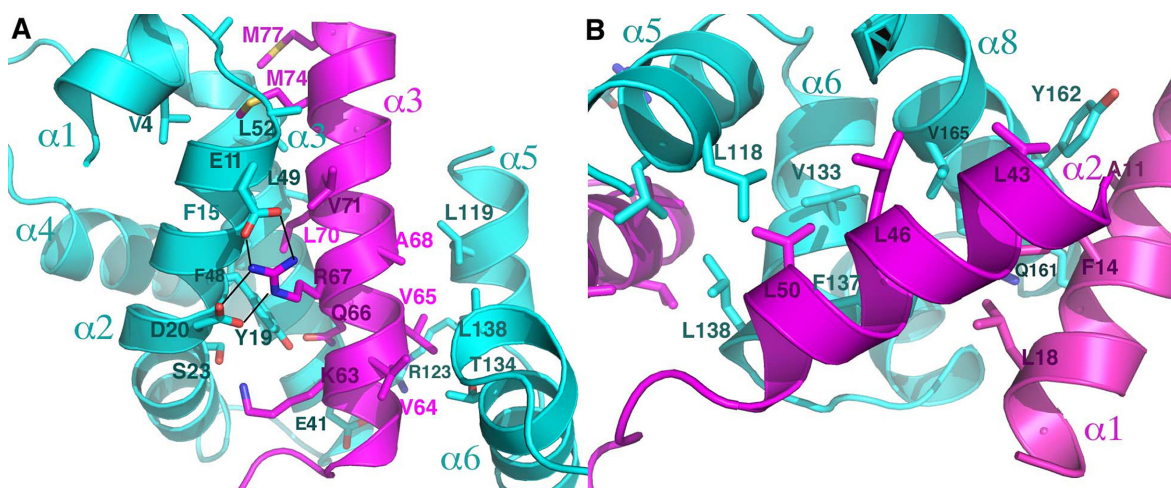


Figure 3. RsbN–BldN interacting interfaces. (A) Shown is a cartoon of RsbN–BldN (colored as in Figure 2) around RsbN $\alpha 3$. RsbN and BldN residues that interact are shown as sticks and labeled. (B) RsbN–BldN interface involving contacts between RsbN $\alpha 1$ – $\alpha 2$ and BldN $\sigma 4$.

is fully encased by helices 1–3 from σ_2 and helices 5 and 6 from σ_4 in these interfaces (Figures 2C–D and 3A). Interactions between RsbN and σ_4 are mediated by RsbN residues Val64, Val65 and Ala68, which sit in a hydrophobic pocket composed of residues Leu19 from σ_4 helix 5 and Thr134 and Leu138 from σ_4 helix 6 (Figures 2D and 3A). In the RsbN– σ_2 interface, σ_2 contacts the RsbN $\alpha 3$ along its entire length, employing mostly hydrophobic contacts, with a few polar interactions around the edges of the interface. Key hydrophobic contacts are formed between RsbN $\alpha 3$ residues Leu70, Val71, Met74 and Met77 and BldN σ_2 residues Val4, Ala12, Phe15, Tyr19, Phe48 and Leu52 (Figure 3A). Polar contacts are mediated between RsbN residues Lys63 and Gln66 and BldN σ_2 residues Ser23 and Tyr19, respectively. RsbN residue Arg67 also makes salt bridge interactions with two BldN σ_2 acidic residues, Glu11 and Asp20 (Figure 3A).

The third RsbN–BldN interface is formed by interactions between RsbN helices 1 and 2 ($\alpha 1$ – $\alpha 2$) and BldN $\sigma 4$ and buries 1560 Å². This interface is also primarily hydrophobic and comprised of contacts between RsbN residues that insert into a shallow crevice formed between BldN $\sigma 4$ helices 5–6 and helix 8 (Figure 3B). A key anchor in this interface is provided by RsbN $\alpha 2$ residue Leu50, which fits into the hydrophobic cavity formed by BldN residues Leu118, Val133, Phe137 and Leu138. $\sigma 4$ residue Phe137 makes van der Waals contacts with RsbN residues Phe14 and Leu18, which are located on RsbN $\alpha 1$. RsbN Phe14 also stacks between $\sigma 4$ residues Gln161 and Tyr162 and RsbN residue Ala11 interacts with Tyr162. Finally, $\sigma 4$ residue Val165 makes hydrophobic interactions with RsbN residues Leu43 and Leu46 (Figure 3B).

Sequence similarity searches indicate that RsbN homologs appear to be found only in *Streptomyces*. Specifically, each sequenced *Streptomyces* genome has a single RsbN homolog, always encoded next to the *bldN* gene. However, even these likely functional RsbN orthologs show a low degree of sequence similarity (Figure 4 and Supplementary Figure S3). Thus, it is notable that the RsbN residues shown to form the three helices that interact with

BldN in the RsbN–BldN crystal structure are highly conserved in length and specific RsbN residues that make direct contacts with BldN in the structure are also conserved (Figure 4 and Supplementary Figure S3). In particular Leu70, which makes a central anchoring contact linking RsbN $\alpha 3$ with BldN $\sigma 2$. Also, RsbN residue Arg67, which makes two salt bridges with BldN acidic residues is completely conserved while RsbN residues located in helices 1, 2 and 3 that make hydrophobic contacts to BldN are highly conserved.

Regulation of BldN by RsbN

Although there are currently no structures of an RNAP–ECF σ holoenzyme complex, either in the presence or absence of DNA, structures of RNAP with other σ factors bound to promoter DNA have shown that in order for σ_2 and σ_4 to simultaneously contact the –10 and –35 promoter elements, respectively, the σ factor must adopt an extended structure (1). In this conformation, the σ_2 and σ_4 domains are separated by more than 80 Å (1,11). In complex with RsbN, BldN assumes a compact conformation with σ_2 and σ_4 juxtaposed, which would prevent simultaneous contact with –10 and –35 elements. Hence, freezing BldN into a compressed shape is one way in which RsbN inhibits BldN activity. High resolution structures of σ_2 and σ_4 bound to their cognate –10 and –35 DNA elements have been solved and can be used to analyze the effects of RsbN on DNA binding by BldN (1,6,8). Overlaying BldN σ_2 onto *E. coli* σ^{E_2} bound to its –10 element (6) shows that RsbN does not clash with the DNA (Figure 5A). In contrast, superimposition of BldN σ_4 onto *E. coli* σ^{E_4} bound to its –35 element shows that binding RsbN would prevent the BldN σ_4 domain from binding its –35 element due to a steric clash between RsbN $\alpha 1$ and the DNA (Figure 5B). Transcription initiation by ECF σ factors requires that both σ_2 and σ_4 bind their cognate –10 and –35 DNA sequences (1,49), and so preventing binding to the –35 element alone would be sufficient to prevent BldN from initiating transcription. Thus, the data indicate that RsbN prevents BldN from functioning as a σ factor through multiple mechanisms. First,

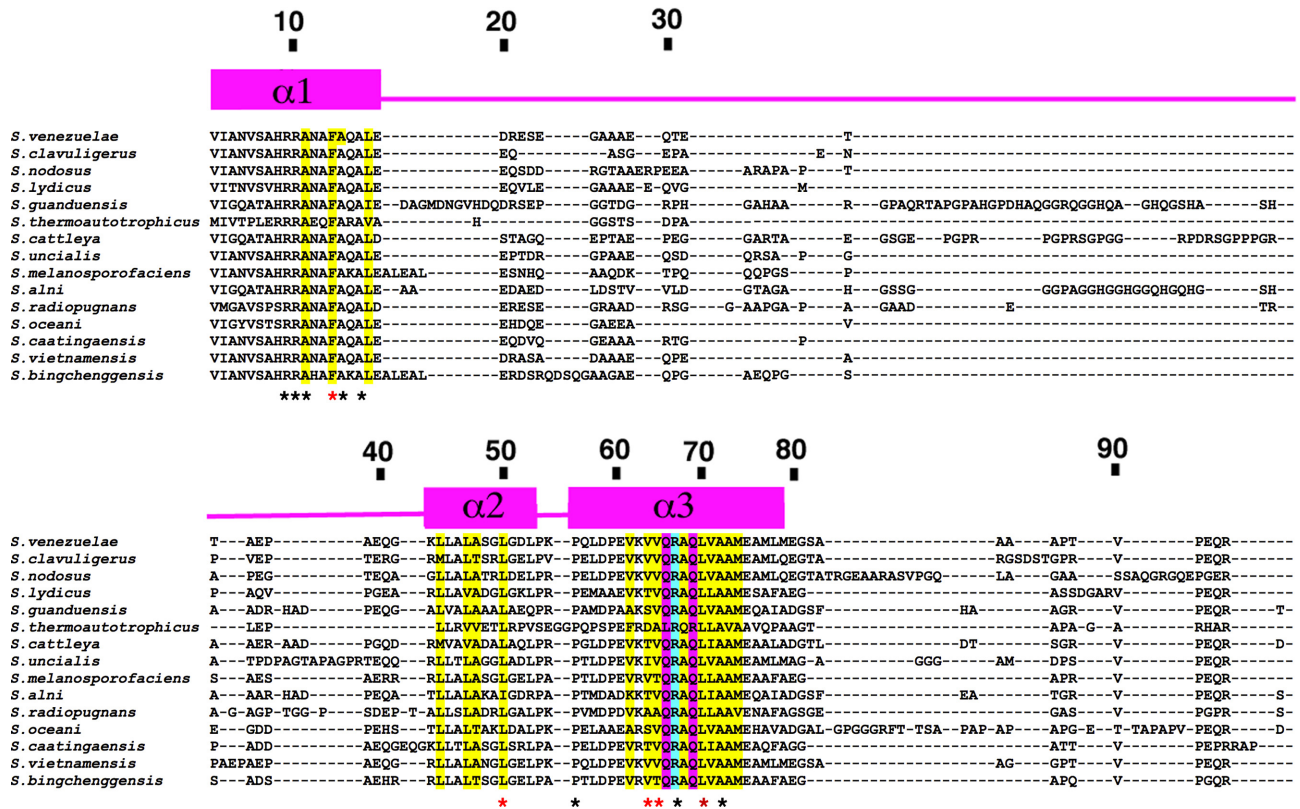


Figure 4. Sequence alignment of the cytoplasmic anti- σ domains of select *Streptomyces* RsbN homologs. Helices revealed in the structure are indicated over the sequences. Black asterisks denote residues that are 100% conserved, while red asterisks indicate conserved residues indicated to be involved in complex formation in the structure and chosen for mutagenesis experiments. Residues that make hydrophobic, polar and salt bridge interactions with BldN are colored yellow, magenta and cyan, respectively. Residues numbers for *Streptomyces venezuelae* RsbN are shown above the alignments. Note that the helical regions, while not completely conserved in sequence between homologs, are conserved in length. RsbN homologs were aligned using the program Kalign, provided as a web service by the EBI (<https://www.ebi.ac.uk/Tools/msa/kalign>).

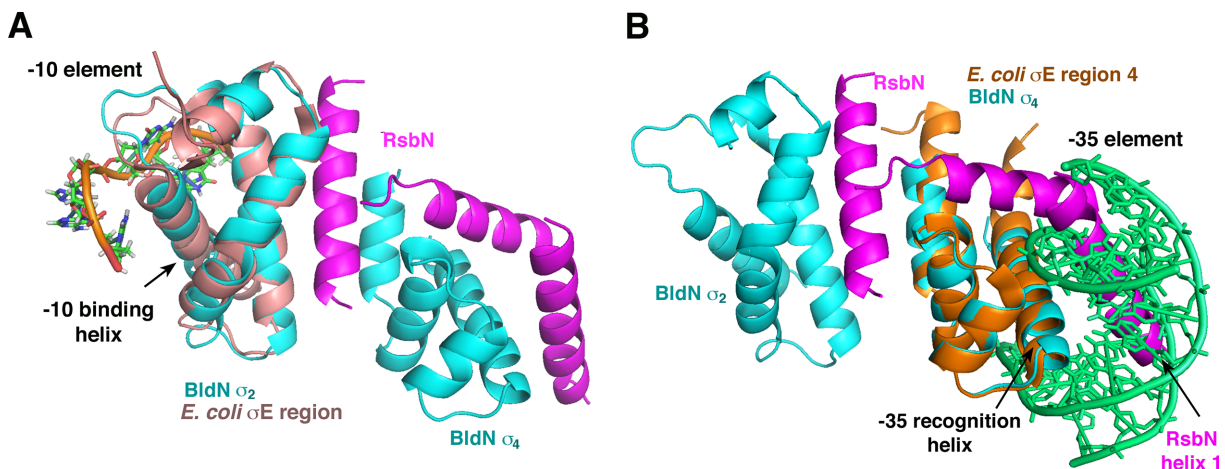


Figure 5. BldN inhibition by RsbN. (A) Overlay of BldN σ_2 onto that of the *Escherichia coli* σ^{E_2} bound to its cognate -10 sequence (4LUP), indicating that RsbN would not impede BldN σ_2 from binding to its -10 promoter element. (B) Superimposition of BldN σ_4 onto *E. coli* σ^{E_4} bound to its cognate -35 element (2H27), which shows that RsbN $\alpha 1$ would clash with the DNA, preventing BldN σ_4 from binding the -35 promoter element.

RsbN binding locks BldN into a compact shape, preventing it from assuming the conformation needed to bind RNAP and the -10 and -35 promoter elements. Second, RsbN binding directly blocks access of BldN domain σ_4 to its -35 promoter element. And third, because RsbN is a transmembrane protein, complex formation with BldN sequesters the σ factor to the membrane.

RsbN structure defines a new family of anti- σ proteins

Although ECF anti- σ factors display low levels of sequence similarity, the structures of these proteins that have been solved to date reveal two classes of anti- σ factors. The most commonly observed anti- σ factor domain (ASD) is a three-helix bundle fold followed by a short helix, termed the class I ASD (12,18,21–26). This type of ASD can be readily detected by DALI searches, which show that the three-helix bundles of representative class I ECF anti- σ factors RseA, ChrR, RsiW and RskA can be superimposed with rmsds ranging from 2.0 Å to 2.6 Å (Figure 6). The second type of ASD is exemplified by CnrY and NepR, which form a small two helix clamp, called the class II ASD (12,26–28) (Figure 6). Our RsbN–BldN structure indicates that RsbN differs from both these types of ASD, revealing it to be the founding member of a new structural class of ECF anti- σ , herein termed the class III ASD (Figure 6). Sequence similarity searches suggest that RsbN anti- σ factors are widespread in *Streptomyces* but appear to be limited to these bacteria and as noted, these alignments show that regions corresponding to the three helices in RsbN are conserved while the linker regions are widely variable (Figure 4). The residues that contact BldN are also conserved (Figure 4 and Supplementary Figure S3). These findings suggest that all RsbN homologs are likely to adopt the same fold and interact similarly with their partner BldN proteins.

Probing the RsbN–BldN structural model

The RsbN–BldN structure revealed a novel σ –anti- σ complex. To test the structural model, we co-expressed truncated versions of BldN and RsbN to examine interactions between individual domains. First, we co-expressed the N-terminally his-tagged version of the RsbN anti- σ domain (RsbN91) with just σ_2 or σ_4 , and found by cobalt affinity purification that RsbN91 can form a stable complex with σ_2 or σ_4 in isolation (Figure 7A, lanes 1 and 2). Control experiments showed that non-his-tagged versions of BldN σ_2 and σ_4 did not interact with the CoCl_2 charged Hi-Trap columns (Supplementary Figure S4, lanes 3 and 4). In the structure of the RsbN–BldN complex, RsbN α_3 is sandwiched between σ_2 and σ_4 (Figure 2C and D). To assess its importance, we co-expressed an N-terminally his-tagged version of RsbN α_3 alone and found that, by itself, RsbN α_3 is sufficient to form a stable complex with BldN (Figure 7A, lane 3). We took this analysis one step further by co-expressing his-tagged RsbN α_3 with either σ_2 or σ_4 in isolation and found that RsbN α_3 forms a stable complex with σ_2 (Figure 7A, lane 4) but not with σ_4 (Supplementary Figure S4, lane 1), showing that the RsbN α_3 interaction with σ_4 is not enough to form a stable complex without additional contacts from σ_2 . In addition, we found that RsbN

α_1 – α_2 alone could not support complex formation with σ_4 (Supplementary Figure S4, lane 2). These studies suggest that the combined interaction interfaces are required for tight complex formation between RsbN and BldN.

The structural data, combined with our biochemical experiments, suggest that three contact points in the RsbN–BldN structure likely cooperate to form a stable complex. Moreover, they suggest that RsbN α_3 forms the lynchpin of the complex between the BldN-interacting region of RsbN and BldN, with α_1 – α_2 maximizing binding via interaction with σ_4 . To probe the structural model in more detail, we tested the effect of mutating residues that the structure suggests would be central to complex formation. Our data showed that BldN σ_4 alone cannot form a stable complex with RsbN α_3 (Supplementary Figure S4, lane 1). However, the structure suggests that BldN σ_2 and σ_4 function together to form a tight complex with RsbN α_3 . If that is the case, we hypothesized that destabilization of the RsbN α_3 interaction with σ_4 may disrupt the more stable RsbN α_3 – σ_2 interaction and prevent the overall RsbN α_3 –BldN interaction. To test this prediction, we generated an MBP–RsbN α_3 fusion protein and co-expressed it with WT BldN. As expected, the construct encoding WT MBP–RsbN α_3 formed a tight interaction with BldN and eluted from SEC at a MW of 67 kDa, consistent with a 1:1 WT MBP–RsbN α_3 –BldN complex (the expected MW is 69 kDa). However, when we mutated RsbN α_3 residues Val64 and Val65 (which the structure indicates are important in mediating the α_3 – σ_4 interaction) to lysine, the interaction between the MBP–RsbN α_3 (V64K–V65K) protein and BldN was clearly disrupted, resulting in two peaks; one containing BldN (at a MW of 26 kDa compared to the expected MW of 21 kDa) and one consisting of MBP–RsbN α_3 (V64K–V65K) at a MW of 47 kDa (compared to the expected MW of the MBP–RsbN α_3 protein of 48 kDa) (Supplementary Figure S5). While there was less soluble BldN when expressed with MBP–RsbN α_3 (V64K–V65K), the soluble BldN present was sufficient to assess complex formation with the mutant MBP–RsbN helix 3 protein. The fact that the mutations in RsbN helix 3 prevented tight complex formation with BldN suggests that the interaction observed between RsbN α_3 and BldN σ_4 observed in the structure is also found in solution.

We next probed the RsbN α_3 –BldN σ_2 and RsbN α_1 – α_2 –BldN σ_4 interfaces. The structure suggests that RsbN residue Leu70 plays a central anchoring role in the interaction of RsbN α_3 with BldN σ_2 (Figure 3A). Leu70 is completely conserved in RsbN homologs and in the structure it inserts into a hydrophobic pocket of BldN σ_2 . We thus replaced Leu70 in RsbN91 with a large, charged arginine side chain and assessed its ability to form a complex with BldN σ_2 . Strikingly, whereas WT RsbN91 bound BldN σ_2 , the mutant RsbN91(L70R) showed no interaction with BldN σ_2 , supporting our structural information (Figure 7B, lanes 1 and 2). To assess the RsbN α_1 – α_2 interaction with BldN σ_4 , we substituted RsbN91 residues Phe14 and Leu50, which are highly conserved and in the structure serve as key points of contact with a surface-exposed hydrophobic pocket in σ_4 . Phe14 and Leu50 were changed to arginine residues and the interaction of the resulting RsbN91 proteins with BldN σ_4 was analyzed. Unlike WT RsbN91, the

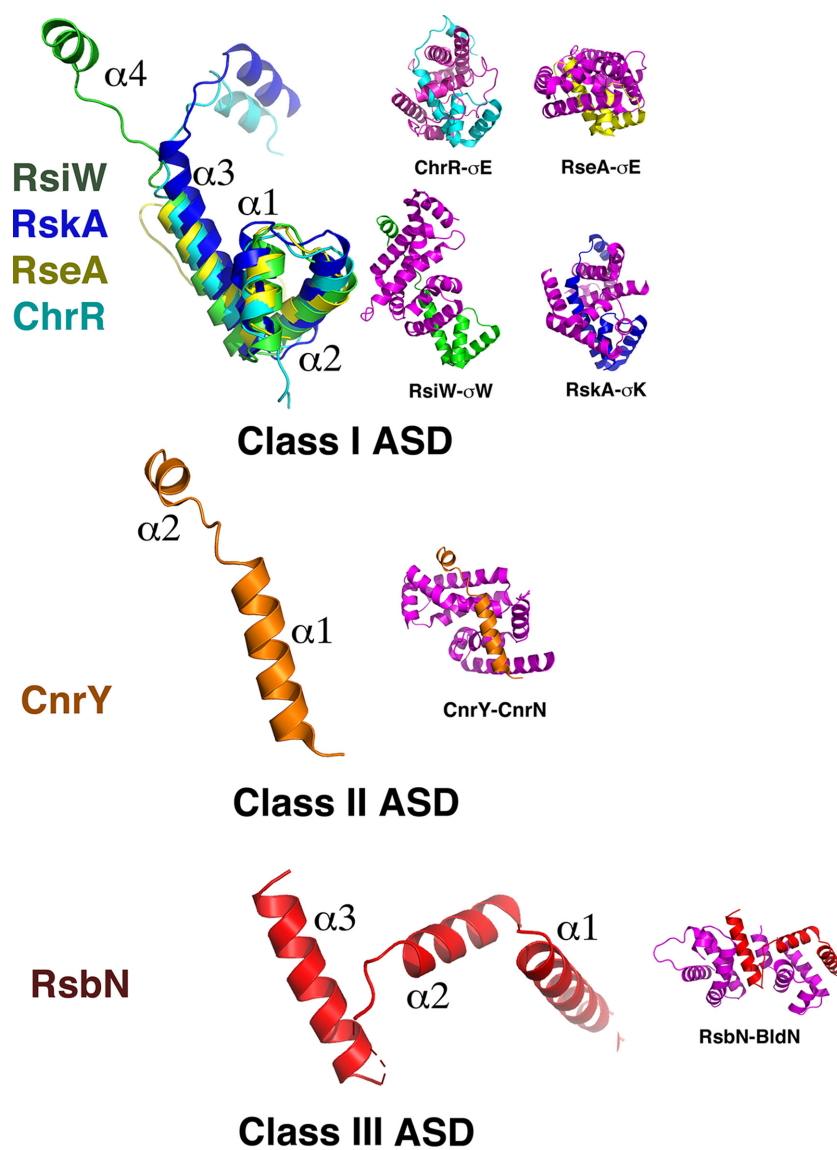


Figure 6. RsbN structure reveals a new type of anti- σ factor fold (ASD). Previously characterized anti- σ ASD folds include the class I ASDs as exemplified by the anti- σ factors RsiW, RseA, ChrR and RskA. These ASDs can be superimposed with rmsds of 2.0–2.6 Å. This ASD is composed of a three-helix bundle structure followed by a fourth helix. Right, shows cartoon representations for these anti- σ factors (in the same orientation as the ASDs on the left) with their bound σ factor. The class II ASDs include CnrY, which consists of a two-helix clamp that surrounds its σ factor (right). RsbN shows no structural homology to the class I or class II ASDs and thus represents a new ASD class, herein termed class III. Shown to the right is its complex with BldN.

mutant protein failed to form a complex with BldN σ_4 (Figure 7B, lanes 3 and 4). BldN σ_2 and σ_4 regions were found in the clarified lysates when expressed with these RsbN mutants, indicating that the lack of binding with the mutant proteins was not due to their insolubility. Thus, our mutagenesis studies provide strong support for all three interfaces observed in the crystal structure.

DISCUSSION

Streptomyces are a biomedically important group of bacteria and serve as a major source of antibiotics and other clinically important compounds. The generation of these ‘secondary metabolites’ coincides with the onset of differentiation. Here we analyzed a protein complex that plays a

central role in controlling this developmental process, the BldN–RsbN complex. BldN is an ECF σ factor whose activity is controlled by an interaction with its cognate anti- σ factor, RsbN, a single-pass membrane protein that has an N-terminal cytoplasmic BldN-binding domain and a large C-terminal extracytoplasmic domain of unknown function (Figure 1) (31). Interestingly, RsbN shows no sequence similarity to any known anti- σ factor or any known protein. To determine the mechanism by which RsbN regulates BldN, here we elucidated the structure of BldN bound to the anti- σ domain of RsbN to 2.23 Å resolution. The RsbN–BldN structure shows that the RsbN anti- σ factor domain contains a fold distinct from other structurally studied anti- σ factors. The structure shows that this RsbN anti- σ domain

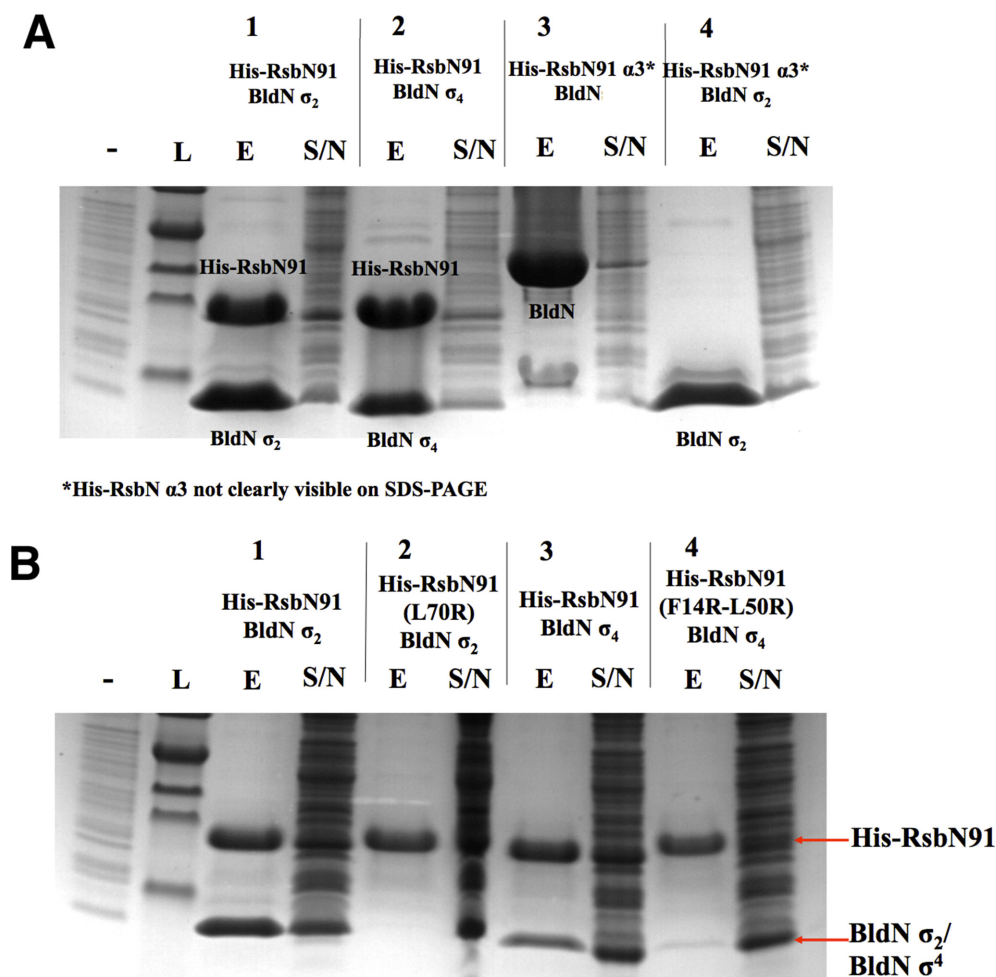


Figure 7. Mutagenesis and biochemical test of the RsbN–BldN structure. (A) Complex formation between his-tagged RsbN91 and σ_2 (lane 1), his-tagged RsbN91 and σ_4 (lane 2), his-tagged RsbN $\alpha 3$ and BldN (lane 3), and his-tagged RsbN $\alpha 3$ and σ_2 (lane 4). Proteins were co-expressed in *Escherichia coli*, purified over a cobalt affinity column, run on a 16% polyacrylamide tricine SDS gel (47) and stained with Coomassie Brilliant Blue. The identities of all proteins were confirmed by MALDI-MS. Note that his-tagged RsbN $\alpha 3$ is not visible in lanes 3 and 4. (B) Complex formation occurs between his-tagged RsbN91 and σ_2 (lane 1) but not between the RsbN91(L70R) variant and σ_2 (lane 2). Complex formation also occurs between his-tagged RsbN91 and σ_4 (lane 3) but not between the RsbN91(F14R-L50R) variant and σ_4 (lane 4). Proteins were co-expressed in *E. coli*, purified using HIS-select spin columns (Sigma H7787), run on a 16% polyacrylamide tricine SDS gel (47) and stained with Coomassie Brilliant Blue. In both A and B the eluted fractions (E) are shown next to the corresponding clarified supernatants (S/N), which thus represents the soluble material obtained after centrifugation. A clarified supernatant from a strain that does not express either RsbN or BldN is also shown (–), next to the protein ladder (L).

interacts with BldN at three distinct interfaces; RsbN $\alpha 3$ contacts both the σ_2 and σ_4 domains of BldN to form two of the interfaces, while RsbN $\alpha 1$ – $\alpha 2$ interact with the BldN σ_4 domain.

Our mutagenesis studies support that the three interfaces revealed in the RsbN–BldN crystal structure are key for complex formation. These interfaces all involve primarily hydrophobic contacts between BldN and RsbN. Interestingly, a detailed examination of the ECF σ –anti- σ structures solved to date reveals that, while these complexes are distinct in their overall structures, the anti- σ factors all make hydrophobic interactions with the same three σ contact points seen in the RsbN–BldN structure. For example, in all these structures a helical region of the anti- σ factor interacts with a hydrophobic region on the σ_2 domain between helices 2 and 3 (using BldN helix numbering) (Figure 8). Interestingly, though all these interactions involve an

anti- σ helical region, how the helix interacts in these complexes is variable; $\alpha 3$ from RsbN and ChrR dock with σ_2 in an N-terminal to C-terminal orientation, RseA binds σ_2 via a C-terminal to N-terminal docking mode and both RskA and RsiW use their $\alpha 4$ helices (not $\alpha 3$) to interact with σ_2 . The other two hydrophobic contact points between the σ and anti- σ factors involve σ_4 regions $\alpha 5$ – $\alpha 6$ – $\alpha 8$ and $\alpha 5$ – $\alpha 6$. In the RsbN–BldN structure the hydrophobic patch in the BldN $\alpha 5$ – $\alpha 6$ – $\alpha 8$ region forms a complementary interface with RsbN $\alpha 1$ – $\alpha 2$. Similarly, in the other ECF σ –anti- σ structures the corresponding region in σ_4 is shielded from solvent by helices of the corresponding anti- σ factor. The specific types of interactions in the structures differ but all shield this hydrophobic region of their σ (Figure 8). Finally, the exposed hydrophobic pocket between $\alpha 5$ – $\alpha 6$ of BldN σ_4 , which is complexed with RsbN $\alpha 3$ in the RsbN–BldN structure, is also protected from solvent in the other σ –anti-

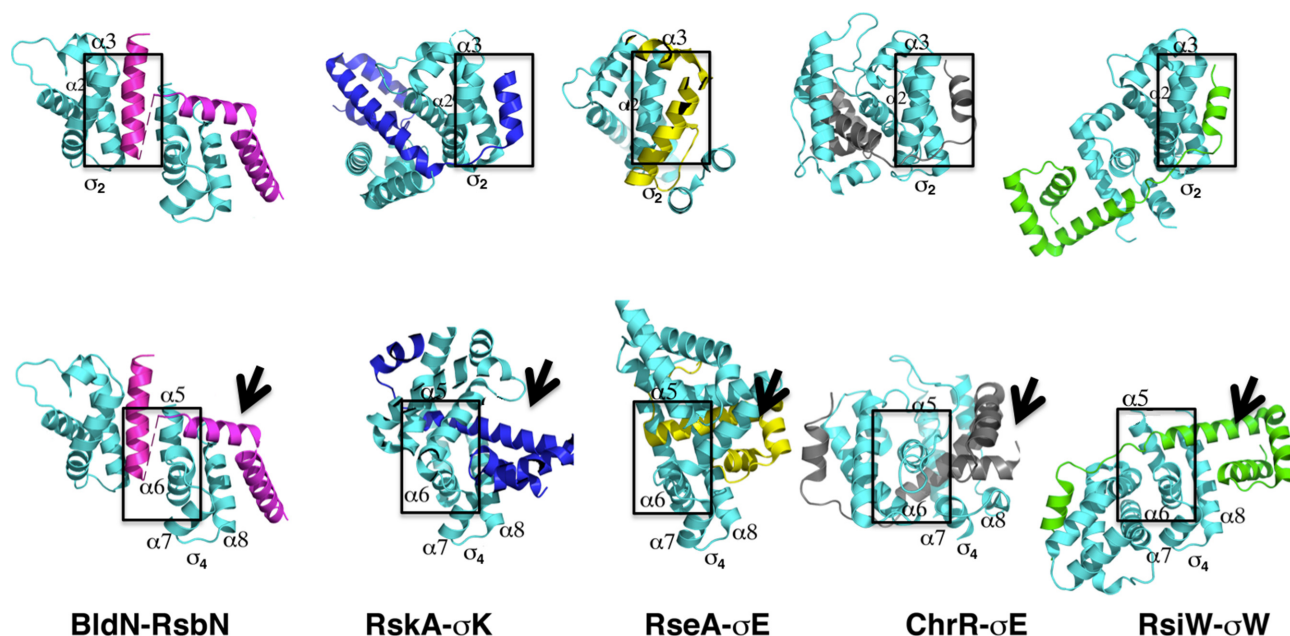


Figure 8. Comparison of σ -anti- σ interfaces. Top row shows comparison of RsbN-BldN with other σ -anti- σ structures with the σ_2 domains shown in the same orientation. Boxed is the hydrophobic region of contact between RsbN (magenta) and BldN (cyan). The same region is boxed in the other σ -anti- σ structures, revealing that all share a σ -anti- σ contact interface involving the burial of the α_2 - α_3 hydrophobic patch on σ_2 . Bottom row shows the σ -anti- σ structures with their σ_4 domains in the same orientation. The interface region formed between RsbN α_3 and RsbN helices 5-6 is boxed as are the corresponding regions in the other σ -anti- σ complexes. In the latter structures, the hydrophobic patch in the σ_4 is similar to the RsbN-BldN structure, covered by anti- σ factor regions and in some cases additional contacts are provided to this σ_4 region by σ_2 . An arrow indicates the contact region between BldN helices α_5 - α_6 - α_8 with α_1 - α_2 of RsbN. Arrows point to the same region of the σ -anti- σ structures to the right of the RsbN-BldN structure showing that these anti- σ factors also contact the homologous region in their partner σ factors. These comparisons thus underscore a general conservation of hydrophobic contact points shared by the σ -anti- σ complexes despite the differences in the structural details of the interactions.

σ structures but by both the anti- σ factor and regions of σ_2 (Figure 8). Thus, these analyses suggest that while σ -anti- σ complexes differ in detail, they appear to share hydrophobic contact points.

One result of the multiple σ -anti- σ contacts is that the complexes all assume an overall compact shape. As binding to RNAP requires the σ factor to adopt an extended conformation, this is one facet of the inhibitory role played by anti- σ factors. Anti- σ factor binding in these complexes also directly inhibits binding of the σ factor to RNAP and/or promoter DNA. Therefore, the anti- σ factor must be inactivated to allow σ factor release and transcription of its target genes. The molecular mechanism underlying the release of BldN from RsbN has not been investigated, but by analogy with *E. coli* RseA- σ^E (50), *Bacillus* RsiW- σ^W (51) and *Bacillus* RsiV- σ^V (52), it seems likely that the inactivation of RsbN will involve a process known as regulated intramembrane proteolysis (18,53,54). The signal that triggers RsbN inactivation is also unclear, but given the bulk of RsbN (residues 140-412) lies on the outside of the membrane, that signal will probably be extracytoplasmic. An attractive but speculative possibility is that this signal is the assembly of the hydrophobic sheath itself, which would create a positive feedback loop to reinforce sheath assembly once it has started.

DATA AVAILABILITY

Coordinates and structure factor amplitudes for the RsbN-BldN complex have been deposited with the Protein Data Bank under the Accession code 6C03.

SUPPLEMENTARY DATA

Supplementary Data are available at NAR Online.

ACKNOWLEDGEMENTS

We thank Susan Schlimpert and Ray Dixon for help with figures, Gerhard Saalbach for MALDI-MS identification of proteins and Chinnam Naga Babu for early work on RsbN-BldN purifications. We also acknowledge Dr Elizabeth A. Campbell and Beth Davis for early proteolysis experiments defining the BldN binding region in RsbN. We acknowledge the Advanced Light Source (ALS) beamline 8.3.1 for data collection with a special thanks to Jane Tanamachi.

FUNDING

National Institutes of Health [GM115547 to M.A.S.]; Biotechnology and Biological Sciences Research Council [BB/N006852/1, BB/L019825/1 to M.J.B.]; Biotechnology and Biological Sciences Research Council Institute Strategic Programme [BB/J004561/1]; National Institutes of Health (in part); National Institute of General Medical Sciences (in part); Howard Hughes Medical Institute; Director, Office of Science, Office of Basic Energy Sciences,

of the U.S. Department of Energy [DE-AC02-05CH11231]; University of California Office of the President, Multi-campus Research Programs and Initiatives Grant [MR-15-328599]; Sandler Foundation (in part). The open access publication charge for this paper has been waived by Oxford University Press - *NAR* Editorial Board members are entitled to one free paper per year in recognition of their work on behalf of the journal.

Conflict of interest statement. None declared.

REFERENCES

- Feklistov, A., Sharon, B.D., Darst, S.A. and Gross, C.A. (2014) Bacterial sigma factors: a historical, structural, and genomic perspective. *Annu. Rev. Microbiol.*, **68**, 357–376.
- Mooney, R.A., Darst, S.A. and Landick, R. (2005) Sigma and RNA polymerase: an on-again, off-again relationship? *Mol. Cell*, **20**, 335–345.
- Gruber, T.M. and Gross, C.A. (2003) Multiple sigma subunits and the partitioning of bacterial transcription space. *Annu. Rev. Microbiol.*, **57**, 441–466.
- Murakami, K.S. and Darst, S.A. (2003) Bacterial RNA polymerases: the whole story. *Curr. Opin. Struct. Biol.*, **13**, 31–39.
- Lonetto, M., Gribskov, M. and Gross, C.A. (1992) The sigma 70 family: sequence conservation and evolutionary relationships. *J. Bacteriol.*, **174**, 3843–3849.
- Campagne, S., Marsh, M.E., Capitani, G., Vorholt, J.A. and Allain, F.H. (2014) Structural basis for -10 promoter element melting by environmentally induced sigma factors. *Nat. Struct. Mol. Biol.*, **21**, 269–276.
- Campbell, E.A., Muzzin, O., Chlenov, M., Sun, J.L., Olson, A., Weinman, O., Trester-Zedlitz, M.L. and Darst, S.A. (2002) Structure of the bacterial RNA polymerase promoter specificity σ subunit. *Mol. Cell*, **9**, 527–539.
- Lane, W.J. and Darst, S.A. (2006) The structural basis for promoter -35 element recognition by the group IV sigma factors. *PLoS Biol.*, **4**, e269.
- Feklistov, A. and Darst, S.A. (2011) Structural basis for promoter -10 element recognition by the bacterial RNA polymerase sigma subunit. *Cell*, **147**, 1257–1269.
- Murakami, K.S., Masuda, S. and Darst, S.A. (2002) Structural basis of transcription initiation: RNA polymerase holoenzyme at 4 Å resolution. *Science*, **296**, 1280–1284.
- Murakami, K.S., Masuda, S., Campbell, E.A., Muzzin, O. and Darst, S.A. (2002) Structural basis of transcription initiation: an RNA polymerase holoenzyme-DNA complex. *Science*, **296**, 1285–1290.
- Campagne, S., Allain, F.H. and Vorholt, J.A. (2015) Extra cytoplasmic function sigma factors, recent structural insights into promoter recognition and regulation. *Curr. Opin. Struct. Biol.*, **30**, 71–78.
- Vassilyev, D.G., Sekine, S.-I., Laptchenko, O., Lee, J., Vassilyeva, M.N., Borukhov, S. and Yokoyama, S. (2002) Crystal structure of a bacterial RNA polymerase holoenzyme at 2.6 Å resolution. *Nature*, **417**, 712–719.
- Lonetto, M.A., Brown, K.L., Rudd, K.E. and Buttner, M.J. (1994) Analysis of the *Streptomyces coelicolor sigE* gene reveals the existence of a subfamily of eubacterial RNA polymerase σ factors involved in the regulation of extracytoplasmic functions. *Proc. Natl. Acad. Sci. U.S.A.*, **91**, 7573–7577.
- Helmann, J.D. (2002) The extracytoplasmic function (ECF) sigma factors. *Adv. Microb. Physiol.*, **46**, 47–110.
- Mascher, T. (2013) Signaling diversity and evolution of extracytoplasmic function (ECF) σ factors. *Curr. Opin. Microbiol.*, **16**, 148–155.
- Staroń, A., Sofia, H.J., Dietrich, S., Ulrich, L.E., Liesegang, H. and Mascher, T. (2009) The third pillar of bacterial signal transduction: classification of the extracytoplasmic function (ECF) sigma factor protein family. *Mol. Microbiol.*, **74**, 557–581.
- Sineva, E., Savkina, M. and Ades, S.E. (2017) Themes and variations in gene regulation by extracytoplasmic function (ECF) sigma factors. *Curr. Opin. Microbiol.*, **36**, 128–137.
- Hughes, K.T. and Mathee, K. (1998) The anti-sigma factors. *Annu. Rev. Microbiol.*, **52**, 231–286.
- Helmann, J.D. (1999) Anti-sigma factors. *Curr. Opin. Microbiol.*, **2**, 135–141.
- Campbell, E.A., Westblade, L.F. and Darst, S.A. (2008) Regulation of bacterial RNA polymerase sigma factor activity: a structural perspective. *Curr. Opin. Microbiol.*, **11**, 121–127.
- Campbell, E.A., Tupy, J.L., Gruber, T.M., Wang, S., Sharp, M.M., Gross, C.A. and Darst, S.A. (2003) Crystal structure of *Escherichia coli* σ^E with the cytoplasmic domain of its anti- σ RseA. *Mol. Cell*, **11**, 1067–1078.
- Campbell, E.A., Greenwell, R., Anthony, J.R., Wang, S., Lim, L., Das, K., Sofia, H.J., Donohue, T.J. and Darst, S.A. (2007) A conserved structural module regulates transcriptional responses to diverse stress signals in bacteria. *Mol. Cell*, **27**, 793–805.
- Shukla, J., Gupta, R., Thakur, K.G., Gokhale, R. and Gopal, B. (2014) Structural basis for the redox sensitivity of the *Mycobacterium tuberculosis* SigK-RskA σ -anti- σ complex. *Acta Crystallogr. D Biol. Crystallogr.*, **70**, 1026–1036.
- Devkota, S.R., Kwon, E., Ha, S.C., Chang, H.W. and Kim, D.Y. (2017) Structural insights into the regulation of *Bacillus subtilis* SigW activity by anti-sigma RsiW. *PLoS One*, **12**, e0174284.
- Maillard, A.P., Girard, E., Ziani, W., Petit-Hartlein, L., Kahn, R. and Govès, J. (2014) The crystal structure of the anti- σ factor CnrY in complex with the σ factor CnrH shows a new structural class of anti- σ factors targeting extracellular function σ factors. *J. Mol. Biol.*, **426**, 2313–2327.
- Herrou, J., Rotskoff, G., Luo, Y., Roux, B. and Crosson, S. (2012) Structural basis of a protein partner switch that regulates the general stress response of α -proteobacteria. *Proc. Natl. Acad. Sci. U.S.A.*, **109**, E1415–E1423.
- Campagne, S., Damberger, F.F., Kaczmarczyk, A., Francez-Charlot, A., Allain, F.H.-T. and Vorholt, J.A. (2012) Structural basis for the sigma factor mimicry in the general stress response of Alphaproteobacteria. *Proc. Natl. Acad. Sci. U.S.A.*, **109**, E1405–E1414.
- Hopwood, D.A. (2007) *Streptomyces in Nature and Medicine: the Antibiotic Makers*. Oxford University Press, NY.
- van Wezel, G.P. and McDowall, K.J. (2011) The regulation of the secondary metabolism of *Streptomyces*: new links and experimental advances. *Nat. Prod. Rep.*, **28**, 1311–1333.
- Bibb, M.J., Domonkos, A., Chandra, G. and Buttner, M.J. (2012) Expression of the chaplin and rodlin hydrophobic sheath proteins in *Streptomyces venezuelae* is controlled by σ^{BldN} and a cognate anti-sigma factor, RsbN. *Mol. Microbiol.*, **84**, 1033–1049.
- Tschowri, N., Schumacher, M.A., Schlimpert, S., Chinnam, N.B., Findlay, K.C., Brennan, R.G. and Buttner, M.J. (2014) Tetrameric c-di-GMP mediates effective transcription factor dimerization to control *Streptomyces* development. *Cell*, **158**, 1136–1147.
- Schumacher, M.A., Zeng, W., Findlay, K.C., Buttner, M.J., Brennan, R.G. and Tschowri, N. (2017) The *Streptomyces* master regulator BldD binds c-di-GMP sequentially to create a functional BldD2-(c-diGMP)₄ complex. *Nucleic Acids Res.*, **45**, 6923–6933.
- Flärth, K. and Buttner, M.J. (2009) *Streptomyces* morphogenetics: dissecting differentiation in a filamentous bacterium. *Nat. Rev. Microbiol.*, **7**, 36–49.
- McCormick, J.R. and Flärth, K. (2012) Signals and regulators that govern *Streptomyces* development. *FEMS Microbiol. Rev.*, **36**, 206–231.
- Bush, M.J., Tschowri, N., Schlimpert, S., Flärth, K. and Buttner, M.J. (2015) c-di-GMP signaling and the regulation of developmental transitions in *Streptomyces*. *Nat. Rev. Microbiol.*, **13**, 749–760.
- Elliot, M.A., Karoonuthaisiri, N., Huang, J., Bibb, M.J., Cohen, S.N., Kao, C.M. and Buttner, M.J. (2003) The chaplins: a family of hydrophobic cell-surface proteins involved in aerial mycelium formation in *Streptomyces coelicolor*. *Genes Dev.*, **17**, 1727–1740.
- Claessen, D., Wösten, H.A.B., Keulen, G.V., Faber, O.G., Alves, A.M.C.R., Meijer, W.G. and Dijkhuizen, L. (2002) Two novel homologous proteins of *Streptomyces coelicolor* and *Streptomyces lividans* are involved in the formation of the rodlet layer and mediate attachment to a hydrophobic surface. *Mol. Microbiol.*, **44**, 1483–1492.
- Claessen, D., Rink, R., de Jong, W., Siebring, J., de Vreugd, P., Boersma, F.G., Dijkhuizen, L. and Wösten, H.A.B. (2003) A novel class of secreted hydrophobic proteins is involved in aerial hyphae formation in *Streptomyces coelicolor* by forming amyloid-like fibrils. *Genes Dev.*, **17**, 1714–1726.

40. Claessen, D., Stokroos, I., Deelstra, H.J., Penninga, N.A., Bormann, C., Salas, J.A., Dijkhuizen, L. and Wösten, H.A. (2004) The formation of the rodlet layer of streptomycetes is the result of the interplay between rodlets and chaplins. *Mol. Microbiol.*, **53**, 433–443.
41. Leslie, A.G. (2006) The integration of macromolecular diffraction data. *Acta Crystallogr. D Biol. Crystallogr.*, **62**, 48–57.
42. Evans, P. (2006) Scaling and assessment of data quality. *Acta Crystallogr. D Biol. Crystallogr.*, **62**, 72–82.
43. Patikoglou, G.A., Westblade, L.F., Campbell, E.A., Lamour, V., Lane, W.J. and Darst, S.A. (2007) Crystal structure of the *Escherichia coli* regulator of σ^{70} , Rsd, in complex with σ^{70} domain 4. *J. Mol. Biol.*, **372**, 649–659.
44. Adams, P.D., Afonine, P.V., Bunkoczi, G., Chen, W.B., Davis, I.W., Echols, N., Headd, J.J., Hung, L.W., Kapral, G.J., Grosse-Kunstleve, R.W. *et al.* (2010) PHENIX: a comprehensive Python-based system for macromolecular structure solution. *Acta Crystallogr. D Biol. Crystallogr.*, **66**, 213–221.
45. Jones, A.T., Zou, J.Y., Cowan, S.W. and Kjeldgaard, M. (1991) Improved methods for building protein models in electron density maps and the location of errors in these models. *Acta Crystallogr. A*, **47**, 110–119.
46. Chen, V.B., Arendall, W.B., Headd, J.J., Keedy, D.A., Immormino, R.M., Kapral, G.J., Murray, L.W., Richardson, J.S. and Richardson, D.C. (2010) MolProbity: all-atom structure validation for macromolecular crystallography. *Acta Crystallogr. D Biol. Crystallogr.*, **66**, 12–21.
47. Schagger, H. and von Jagow, G. (1987) Tricine-sodium dodecyl sulfate-polyacrylamide gel electrophoresis for the separation of proteins in the range from 1 to 100 kDa. *Anal. Biochem.*, **166**, 368–379.
48. Ding, F., Prutzman, K.C., Campbell, S.L. and Dokholyan, N.V. (2006) Topological determinants of protein domain swapping. *Structure*, **14**, 5–14.
49. Rhodius, V.A. and Mutalik, V.K. (2010) Predicting strength and function for promoters of the *Escherichia coli* alternative sigma factor σ^E . *Proc. Natl. Acad. Sci. U.S.A.*, **107**, 2854–2859.
50. Alba, B.M., Leeds, J.A., Onufryk, C., Lu, C.Z. and Gross, C.A. (2002) DegS and YaeL participate sequentially in the cleavage of RseA to activate the σ^E -dependent extracytoplasmic stress response. *Genes Dev.*, **16**, 2156–2168.
51. Heinrich, J., Hein, K. and Wiegert, T. (2009) Two proteolytic modules are involved in regulated intramembrane proteolysis of *Bacillus subtilis* RsiW. *Mol. Microbiol.*, **74**, 1412–1426.
52. Hastie, J.L., Williams, K.B. and Ellermeier, C.D. (2013) The activity of σ^V , an extracytoplasmic function σ factor of *Bacillus subtilis*, is controlled by regulated proteolysis of the anti- σ factor RsiV. *J. Bacteriol.*, **195**, 3135–3144.
53. Ades, S.E. (2008) Regulation by destruction: design of the σ^E envelope stress response. *Curr. Opin. Microbiol.*, **11**, 535–540.
54. Ho, T.D. and Ellermeier, C.D. (2012) Extra cytoplasmic function σ factor activation. *Curr. Opin. Microbiol.*, **15**, 182–188.